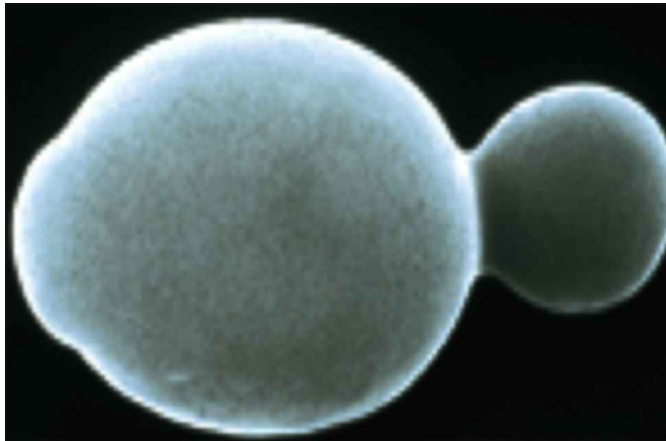


CHALMERS



Simulations of asymmetric segregation of damaged proteins during yeast-cell division

Erasmus Mundus Masters in Complex Systems Science M1 Project

MARTIN ANDRADE RESTREPO

Department of Physics & Engineering Physics
Non-linear Dynamics & Statistical Physics
CHALMERS UNIVERSITY OF TECHNOLOGY
Gothenburg, Sweden 2012
M1 Project 2012:6

Abstract

During yeast-cell division, Hsp104-associated aggregates are distributed unequally between the daughter and the mother cell. Only around three out of ten daughter cells end up having at least one Hsp104 protein after cell division is complete (reference [4]). Although evidence shows that aggregates are dragged away from the bud by the actin cytoskeleton formed in the actin nucleation centers (reference [4]), the exact mechanism causing this asymmetry is yet unknown. In this project different reasons that may explain the abnormal inheritance of damaged proteins were studied. As a starting point, it was assumed that the aggregates undergo a random walk when not encountering obstacles or being subject to the different forces that may hold them inside the mother cell. For this, two-dimensional and three-dimensional simulations were performed of protein aggregates diffusing inside a yeast cell, of protein aggregates diffusing inside a yeast cell with a vacuole and of protein aggregates diffusing inside a yeast cell with both a vacuole and our interpretation of the actin cables' influence in the Hsp104 aggregates' movement. One aim was to study the nature and the source of the experimentally observed anomalous diffusion. In every simulation, the probability of at least one aggregate being present in the daughter after cell division is over was computed in order to verify whether our data agreed with the experimental observations. Our results suggest that the irregular distribution of the Hsp104 aggregates happens due to two effects: the special geometry of the dividing yeast cell in which the aggregates diffuse, and aggregate attachment to actin cables.

Acknowledgements

First of all, I would like to thank Bernhard Mehlig and Thomas Nyström for both their teaching and their constant enthusiasm and patience throughout the time we worked together on the project. I'd also like to thank Erasmus Mundus for the oportunities they've given me as a student of the *Erasmus Mundus Masters in Complex Systems Science* to form myself, not only as a better professional, but as a better individual.

Martín Andrade, Gothenburg, Sweden 25/6/12

Contents

1	Introduction	1
2	Model	4
2.1	Experiments	4
2.2	Diffusion	7
2.2.1	Basic Principles of Diffusion (reference [1])	7
2.2.2	Two-Dimensional Simulations of Diffusion	8
2.2.3	Three-Dimensional Simulations of Diffusion	13
3	Results	15
3.1	Random Walk in x-y Plane	15
3.2	Diffusion Inside a Circle	15
3.3	Diffusion Inside an Annulus	17
3.4	Simulations of Hsp104-Associated Aggregate Diffusion in yeast cytokinesis	18
3.5	Remake of Simulations in [13]	19
3.5.1	Two-dimensional simulations	20
3.5.2	Three-dimensional simulations	21
3.6	Simulations of Hsp104-associated aggregate diffusion in yeast cytokinesis in the presence of actin cytoskeleton	21
3.7	Comparison to Experiments	23
4	Conclusion	25
	Bibliography	29
A	Diffusion in Confined Spaces	30
A.1	Diffusion Equation in Polar Coordinates	30
A.2	Diffusion in the Annulus	31
B	Results from Simulations with the Possibility for the Aggregates to Attach to the Actin Filaments	33

1

Introduction

AGING IN UNICELLULAR ORGANISMS such as yeast cells is strongly associated with cellular division. Cell division in yeast cells gives rise to an “aging” and an “immortal” lineage. The “aging” lineage consists of an old mother cell with a decreased survival rate, while the “immortal” one of a new, healthy daughter cell with a longer life span and full replicative potential. Figures 1.1a) and 1.1b) show the relationship between the survival rate of yeast cells and the number of divisions they undergo, and the comparison between the mean life span of the mother and the daughter cells after budding. Recent observations [4] show that the difference in the average endurance between the two outcomes of yeast cell division is highly connected to the asymmetrical distribution of Hsp-104-associated protein aggregates between them. This is, since oxidized proteins such as Hsp-104-associated aggregates affect the fitness and maintenance of yeast cells. In fact, observations show that, although the average number of Hsp-104-associated aggregates in regular yeast cells is 15, only one of every three daughter cells inherits at least one of them ([4]).

The exact mechanism that causes the asymmetry in the inheritance of Hsp-104-associated aggregates remains unclear. Hence, in the last couple of years, a number of studies such as the ones in [4], [13], and [11] present hypotheses that may explain why the aggregates are kept inside the mother cell.

Recent observations suggest that the actin cytoskeleton of the yeast cells transports, via cable flow, the Hsp-104-associated aggregates towards the mother cell. It seems that, the actin cables (filaments that contribute to the establishment of cell polarity), created in the actin nucleation centers located in the tip of the daughter cell and the neck connecting it to the mother (see figure 1.2), carry the damaged proteins away from the bud as they elongate. It is then considered possible that, due to a chemical reaction between the actin and the Hsp-104-associated protein molecules, the Hsp-104-associated protein aggregates adhere to the actin filaments and therefore move along with them as they

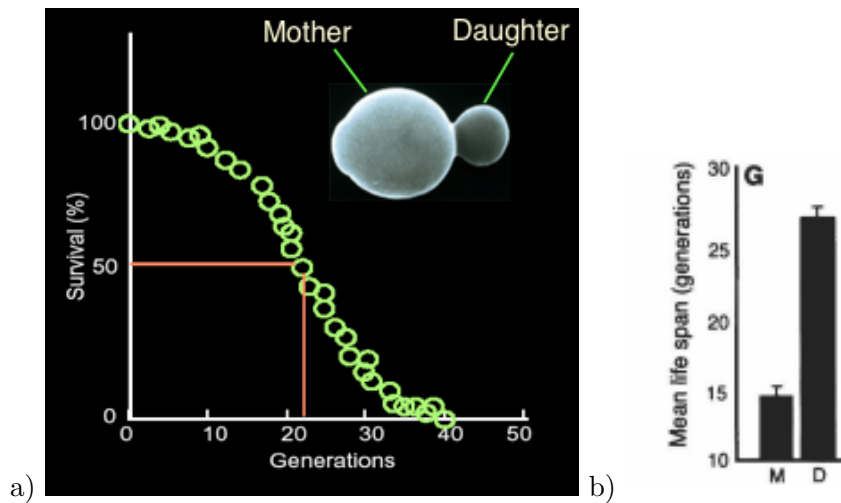


Figure 1.1: a) Relationship between the survival rate and the number of cell divisions in yeast cells. Image taken from [7]. b) Mean life span of the mother and daughter cells. Image taken from [4].

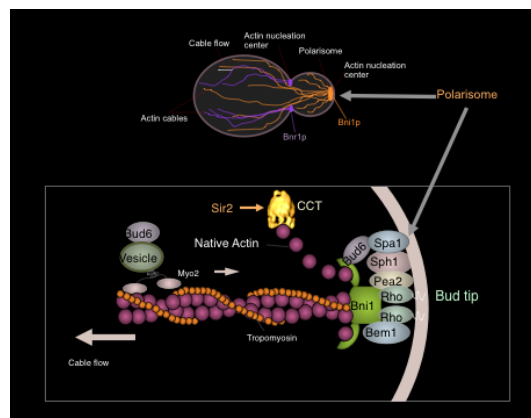


Figure 1.2: Image of the actin cytoskeleton. Image taken from [7].

grow.

The previous hypothesis, however, is not the only one that has been put forward when studying the asymmetrical distribution of damaged proteins. More recently, it was stated that the reason for the Hsp-104-associated protein aggregates to remain inside the mother cell during yeast cell division is likely to be a consequence of both, slow diffusion of the aggregates and the complex geometry in which they lie [13]. Allegedly, when using particle tracking techniques to observe the dynamics of the aggregates, the results suggest that these undergo an unbiased random walk during cell-cycle stages such as cell division. Consequently, aging in yeast cells could be a result of a purely stochastic process.

As a response to this last approach, an explanation of both the anomalous diffusion of the aggregates and the unbalanced distribution of them between the bud and the mother cell, was presented in [11]. The authors of [11] state that the confinement of the Hsp104-associated aggregates to the organellar surfaces inside yeast cells justifies their observed dynamics and their inability to travel inside the daughter cell during yeast cell division. The authors of [11] observed slow-diffusive behavior of the protein aggregates is actually a result of constrained diffusion along the surfaces of organelles such as the vacuole and the IPOD. Hence, instead of being a pure random process, aging is also dependant on the chemical attractions between the organelles' surface and the Hsp104-associated protein aggregates.

The following project is a compilation of the results I obtained when studying, with the aid of numerical simulations, how persuasive some of the previously introduced theories are.

2

Model

TO INVESTIGATE THE DYNAMICS of Hsp-104-associated protein aggregates in budding yeast cells, as in most of the research arising in the field of experimental sciences, the first interaction with the unclear aspects of the aggregates' behavior must be done via direct experimental observation. This approach, however, may be insufficient since properties such as the system's complexity (its parts interact in complicated ways), or the system's size when dealing with macro and microscopical scales, may become obstacles to the comprehension of it. In such cases, numerical approaches become a helpful tool as they can simplify the elusive nature of the system by capturing what seem to be its essential characteristics. In the following sections I will explain in detail both the experimental observations and the numerical simulations important for studying the source of the asymmetry in the Hsp104-associated protein-aggregate distribution during yeast cell division.

2.1 Experiments

The analysis of the dynamics of Hsp-104-associated protein aggregates in yeast cells using modern methods such as particle tracking, show that, unlike regular proteins which diffuse freely, these aggregates are distributed asymmetrically between the daughter and the mother cell during cytokinesis [13]. In fact, most of the aggregates are retained in the mother cell throughout the entire cell division process; only around 30% of the newborn yeast cells inherit one or more damaged protein aggregate [4]. Thus, a number of experimental approaches have aimed to understand, if not the absolute reason for such unequal distribution, the aspects that may or not influence it.

One of the most approved hypotheses that arose on this matter, states that the abnormal distribution of damaged-protein-aggregates depends upon on both the actin cytoskeleton as well as the concentrations of compounds in the cytoplasm. In fact, re-

cent observations ([4]) have shown that sirtuin or *Sir2p* (protein fundamental for cellular regulation in yeast) has a substantial role in both the levels of damaged proteins and their distribution. In fact, mutated yeast cells without *Sir2p*, showed not only a higher concentration of damaged proteins but a more symmetrical distribution during cytokinesis. This was seen when measuring the concentration of damaged proteins in yeast cells lacking both *fob1* (DNA replication fork-blocking protein) and *Sir2p* proteins. In this case, yeast cells were injected with Hsp104p as well as hydrogen peroxide. Hsp104 p, upon a heat shock, accumulates around the aggregates of damaged proteins and glows, making it possible to visualize the aggregates. On the other hand, hydrogen peroxide induces protein aggregation. In the first case (cells lacking *fob1*), the asymmetry of Hsp-104-associated aggregates during yeast budding remained, while in the second (cells lacking *fob1* and *Sir2p*) the amount of damaged protein aggregates found in the bud was twice as much as under regular circumstances. Additionally, as in regular cytokinesis, the non-oxidated proteins showed no particular unequal distribution. Thus, evidence suggests that sirtuin is a crucial element in the distribution of damaged protein aggregates but not in the behavior of all proteins per se.

Another observation made from the same experiment was that damaged, oxidated proteins not only affect negatively the fitness of yeast cells, but shorten their mean life span as well. Indeed, yeast cells with lower levels of *Sir2p* and a larger number of damaged protein aggregates exhibited a shorter life span than those in natural conditions.

Additionally, in the same study [4], the effect of the actin-cytoskeleton on the distribution of damaged proteins was verified experimentally. The formation of the actin-cytoskeleton was suppressed with Latrunculin-A (Lat-A), which binds to the actin molecules impeding them to form the actin filaments. As a matter of fact, Lat-A obliterated completely the segregation of Hsp104-associated proteins in yeast budding. Hence, at first sight, just as sirtuin, the actin cytoskeleton has a strong correlation with the odd behavior of Hsp104-associated protein aggregates during cytokinesis.

The previously described analysis is, however, only one of the possible explanations for the observed dynamics of the damaged-protein aggregates during yeast-cell division. In a recent investigation ([13]), damaged protein aggregates were observed in live yeast cells. They were observed with the use of Hsp104-GFP after the cells were somitted to a 30 minute heat shock at 42°C. When the yeast cells were at a 30°C, they were imaged in 3D and 2D confocal movies. According to them, there is no evidence of aggregate movement from the bud to the mother cell to happend with more regularity than that in the opposite direction. Instead, particles appear to undergo an unbiased random walk with a small amount of confinement (30% of subdiffusion). To show this, the mean squared displacement of the damaged protein aggregates was averaged over 1068 aggregate trajectories, and was compared to numerical simmlations of superdiffusion, diffusion and subdiffusion. The results are shown in [13]. The experimentally observed mean-square-displacement agrees with that of subdiffusion, that is, behaves as

$$\langle r^2 \rangle = 4D_\alpha \tau^\alpha, \quad \alpha < 1 \quad (2.1)$$

where τ is time and D_α is the diffusion constant. This however, is not the expected behavior since, at least at short time scales, superdiffusion ($\alpha > 1$) would occur when the aggregates are actively transported by actin filaments. To verify that the cells observed in the experiment had not randomly mutated in such a way to compromise the dynamics of damaged protein aggregates, the results were compared with those acquired in previous experiments. The trajectories, seen in the other movies, showed to be of the same kind of the measured ones in the experiment.

In response to the experiments conducted in [13], Spokoini et al [11], in their most recent work, made and analysed movies of both protein aggregates and cell organelles such as the IPOD and the vacuole. The movies showed that the dynamics of protein aggregates in budding yeast cells which, as it was said, was classified as subdiffusion, was, apparently, diffusion on the surface of organelles instead. Hence, the dynamics of HSp104 associated aggregates was most likely to be non entirely random.

The results summarized above show that in the study of the asymmetrical distribution of damaged proteins, a number of questions yet remain elusive. The matters that are yet unsolved, remain unclear, or are unconvincing are summarized in the following questions.

- Is the asymmetrical inheritance of damaged protein aggregates in yeast cells dependant influenced by sticking to the actin cytoskeleton?
- Are the damaged protein aggregates undergoing diffusion or anomalous diffusion?

The main question is the following.

- Which mechanism retains the damaged protein aggregates inside the mother cell during yeast cytokinesis?

As the results of the experiments show, despite the fact that such questions have been directly addressed in experiments such as the those in [13], [11], and [4] the conclusions remain ambiguous. For example, though the asymmetric inheritance of damaged proteins appears to depend on the actin filaments [4], the measurement of the mean-square-displacement of them shows no evidence of any biased transport [13]. Hence, in order to address the questions listed above, other mechanisms or approaches can result helpful in solving the persistent uncertainties. For instance, real time three-dimensional tracking of protein aggregates would make it possible to distinguish whether particles are undergoing anomalous diffusion or just diffusion along the surface of the cells organelles. On the other hand, a more detailed visualization of both the actin cytoskeleton and the Hsp104-associated aggregates would probably show if there exists or not a correlation between them.

In this project we used numerical simulations to address the questions listed above. Simulations are advantageous as they can isolate the influence that different parts have on a particular complex system's behavior. This way, by capturing the essential characteristics of a model questions as the one in this project can be studied. This, as simulations

may quantitatively answer how each of the potential mechanisms of aggregate retention influences the asymmetry in their distribution. More explicitly, I used numerical simulations to study how two empirically measured quantities behave in a model incorporating the characteristics that, according to the above publications ([13], [4]), may serve as explanations for the asymmetrical inheritance of Hsp104-associated aggregates during yeast-budding. The measurements are the mean-square-displacement of the aggregates' and the probability of a newborn yeast cell having at least one damaged protein at the end of the cell division process.

2.2 Diffusion

To model the dynamics of the damaged protein aggregates in yeast cells, it was assumed that they diffuse in the cytoplasm. The reason for this assumption, is that experimental observations in microbiology show that proteins and other biologically important aggregates undergo random walks when present in living cells. In the following sub-section the basic principles of diffusion are introduced. Then, the simulations of aggregate diffusion are explained in detail.

2.2.1 Basic Principles of Diffusion (reference [1])

Consider a particle undergoing a random walk in a one spatial dimension, starting at the origin. In every time step of length δt the particle moves, either to the left or to the right, a distance of δx . If the probability of moving to the right is equal to that of moving to the left then the probability $Q(x,t)$ of a particle being in position x after t units of time satisfies the so called 'diffusion equation'

$$\frac{\partial Q}{\partial t} = D \frac{\partial^2 Q}{\partial x^2}. \quad (2.2)$$

where $D = \frac{\delta x^2}{2\delta t}$ is the 'diffusion constant'. This equation is known as the Diffusion Equation, its solution is

$$Q(x,t) = \frac{1}{\sqrt{4\pi Dt}} \exp\left(\frac{-x^2}{4Dt}\right). \quad Q(0,0) = 1. \quad (2.3)$$

Now, consider the transformation to dimensionless variables $x^* = \frac{x}{\sqrt{4Dt}}$, $t^* = ct$. Let $Q^*(x^*,t^*) = Q(x,t)$ Then, the dimensionless form of the law of diffusion can be derived using chain rule,

$$\frac{\partial Q^*}{\partial t^*} = \frac{1}{c} \frac{D}{4Dt} \frac{\partial^2 Q^*}{(\partial x^*)^2}$$

For convenience we let $c = \frac{1}{4t}$ to get

$$\frac{\partial Q^*}{\partial t^*} = \frac{\partial^2 Q^*}{(\partial x^*)^2} \quad (2.4)$$

The quantity that characterises dynamics in diffusion processes is the mean-square-displacement (MSD) $\langle x^2(t) \rangle$ as function of time. Calculating it yields

$$\langle x^2(t) \rangle = \int_{-\infty}^{\infty} x^2 Q(x,t) dx = 2Dt. \quad (2.5)$$

which is known as the Law of Diffusion.

Generalizing to $d \geq 1$ dimensions, if $r(t)$ denotes the Euclidean distance between the initial position of the particle and the position at time t then, considering that the movement in different dimensions is independent,

$$\langle r^2(t) \rangle = \left\langle \sum_{i \leq d} x_i^2 \right\rangle = \sum_{i \leq d} \langle x_i^2 \rangle = 2dDt. \quad (2.6)$$

‘Anomalous diffusion’ by contrast corresponds to the case where

$$\langle r^2(t) \rangle = 2dD_\alpha t^\alpha. \quad (2.7)$$

with $\alpha < 1$ (subdiffusion) or $\alpha > 1$ (superdiffusion).

2.2.2 Two-Dimensional Simulations of Diffusion

It is often assumed that protein aggregates undergo a random walk in the cytoplasm. In this case, their dynamics can be studied in terms of a diffusion process. However, diffusion in cells is obstructed by mobile and immobile obstacles such as the cell walls and the organelles. Hence, the observed mean-square-displacement of the aggregates is unlikely to behave as that observed in regular diffusion of particles as introduced in the previous section. If, moreover, the aggregates are transported by the cytoskeleton, the probabilities of moving in different directions are unequal. This means that, instead of regular diffusion, the damaged proteins’ dynamics would likely resemble anomalous diffusion or directed motion.

As it is explained in detail below, the simulations for this project aim to resemble the observed dynamics of damaged protein aggregates by modelling their diffusion and possibly subdiffusion (in the standard way). Likewise, constraints as the finite size of the domain (mother and daughter cell), the presence of the vacuole (biggest organelle inside the yeast cell), the finite size of the protein aggregates, and the moving boundary of the growing daughter cell are implemented in the two-dimensional and three-dimensional programs. This is done in order to appreciate the influence each one of them has on the mean-square-displacement of the aggregates and to compare to the experimental data available in the figures in [13]. Furthermore, every simulation calculates the probability of the daughter cell having at least one aggregate after cytokinesis is complete to verify if the selected mechanism, besides affecting the aggregates’ mean-square-displacement in the desired way, is successful in generating the asymmetry in the distribution of them

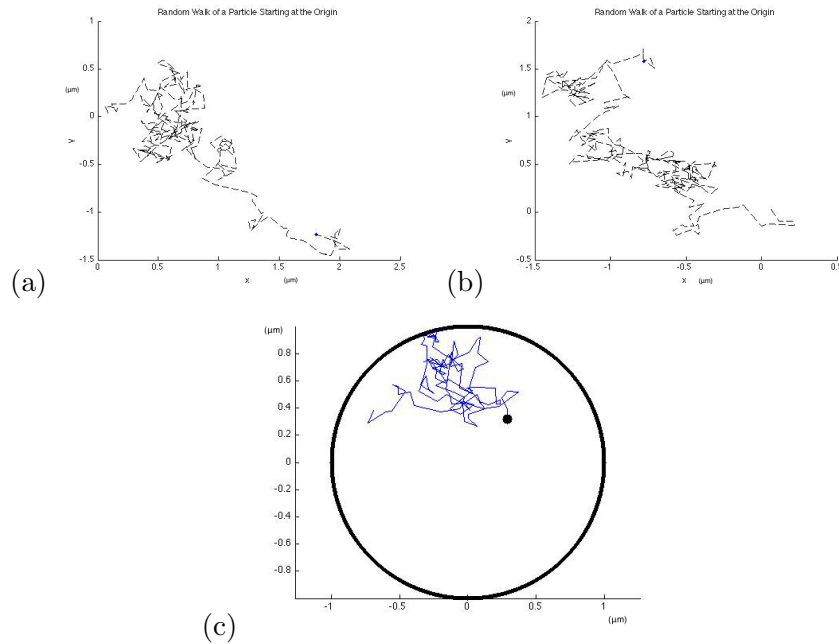


Figure 2.1: (a,b) Trajectories of a particle undergoing a random walk and starting on the origin of the x-y plane. (c) Trajectory of a particle undergoing a random walk inside a circle of radius $1 \mu\text{m}$. In both cases, the diffusion constant D was taken to be $0.0005 \mu\text{m}^2/\text{sec}$ and the time step δt was set to 5sec .

between the bud and the mother cell.

The programming language used for the simulations is MATLAB.

As a first step, simulations of a random walk of a particle in the two-dimensional space and inside a circle were ran. In either case, the particle, initially at the origin, and currently in position (x,y) was moved every time step of size δt to the position $(x + \chi_1, y + \chi_2)$ where χ_1, χ_2 are independent Gaussian-distributed random variables with mean 0 and standard deviation $\sqrt{2D\delta t}$. The diffusion constant D was taken to be $0.0005 \mu\text{m}^2/\text{sec}$ and δt was taken to be 5 seconds. If however, in the case where the particle was confined to diffuse inside the circle, it meant to move outside the circle's boundary, then the particle bounced back with its angle of incidence equal to its angle of reflection as shown in figure 2.2(a). Examples of the trajectories of the particle in different simulations of both programs are shown in figure 2.1.

So far we have only considered an abstract representation of the random walk of aggregates inside yeast cells, where they are represented as nondimensional particles and the cells as perfect circles. Hence, in order to make the program more accurate, the particle was replaced by a disc which represented the aggregate and its finite size. The boundary conditions were adapted in such a way that the distance between the center of the disk (aggregate) and the origin would never be larger than $r_c - r_a$ where r_c denotes

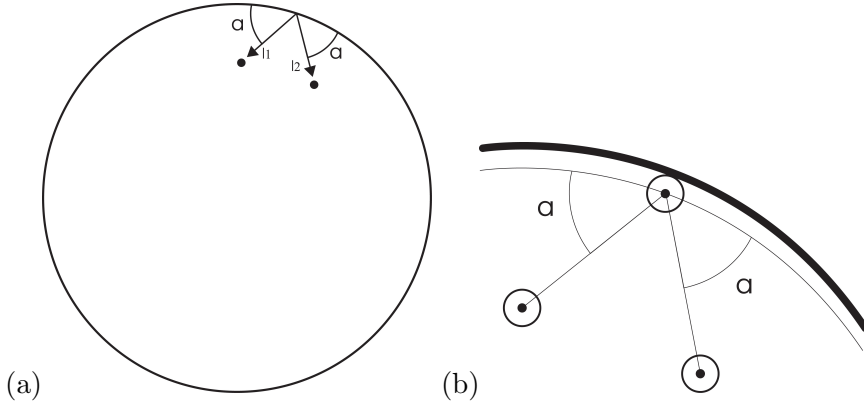


Figure 2.2: (a) Boundary conditions of a particle diffusing inside a circle. Here $l_1 + l_2$ equals the magnitude of the particle's movement. (b) Boundary conditions in the simulation of a protein aggregate diffusing inside a yeast cell.

the radius of the cell and r_a the radius of the aggregate. Thus, the center of the aggregate would behave as the non-dimensional particle considered in the previous program with the difference that the space constraint was no longer a circle with radius $1 \mu\text{m}$ but a circle with radius $r_c - r_a$. For clarity see figure 2.2(b). Additionally, the aggregate's center was initiated randomly in a point (x_0, y_0) inside the circle representing the yeast mother cell. For this x_0 and y_0 were taken as $x_0 = (r_c - r_a)\sqrt{\beta} \cos(\alpha)$ and $y_0 = (r_c - r_a)\sqrt{\beta} \sin(\alpha)$ with β and α random numbers in the intervals $[0,1)$ and $[0,2\pi)$ respectively.

Next, to simulate yeast cytokinesis, the aggregates were allowed to diffuse inside another circle connected to the original one by a neck as it is shown in figure 2.3. This new circle is a representation of the daughter cell. Constraints such as the expanding boundaries of the daughter cell and the vacuole (a circular region inside the mother cell in which the aggregates are not allowed to diffuse) were added both separately and combined (figure 2.4) to study their effect in the aggregates' mean-square-displacement. Recall that the general aim was to seek concordance with the measurements in the experiments performed in [13]. The boundary conditions at the vacuole's surface were identical as those at the cell walls (angle of incidence equal to the angle of reflection). The simulations of budding were also adapted, with and without the constraints, to model subdiffusion of the aggregates. In this case, as done in [13] 30% of the aggregates were not allowed to go further than $0.5 \mu\text{m}$ away from their initial positions. The parameter values that were used for the programs -taken from the experiments performed in [13], [4], and the experimental observations - are listed below.

- Mother's diameter = $5 \mu\text{m}$.
- Daughter's diameter = $3.8 \mu\text{m}$ (At the end of the division process).
- Aggregate's diameter = $0.12 \mu\text{m}$.

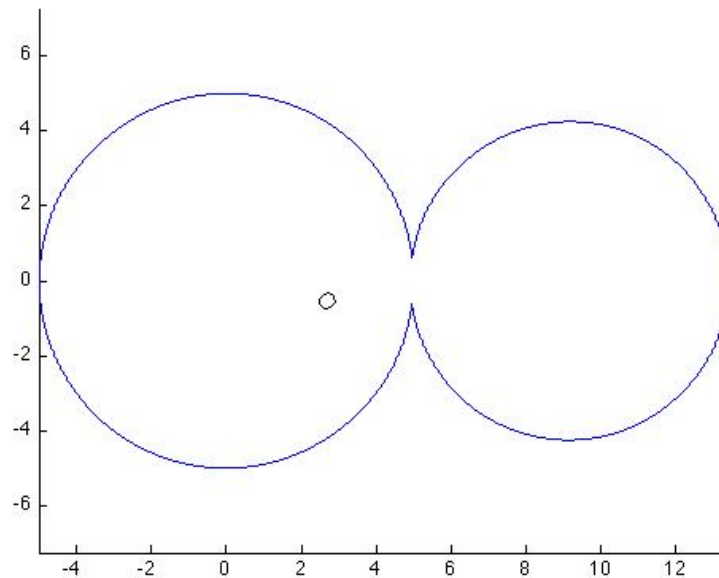


Figure 2.3: $0.12 \mu\text{ m}$ diameter aggregate undergoing a random walk inside a $5 \mu\text{ m}$ cell and $4.5 \mu\text{ m}$ bud connected by a $1.35 \mu\text{ m}$ neck.

- Vacuole's diameter = $2.55 \mu\text{ m}$.
- Neck's length = $1.25\text{-}1.35 \mu\text{ m}$.
- Amount of particles in a cell = Gaussian number with mean $\mu = 15$ and variance $\sigma^2 = 9$.
- Diffusion Constant $D = 0.0005 \mu\text{ m}^2/\text{ s}^2, 0.0008 \mu\text{ m}^2/\text{ s}^2, 0.001 \mu\text{ m}^2/\text{ s}^2$.
- The neck is open during 100 min.

In accordance with the observations done in [4] showing an existing dependence of the Hsp104-associated aggregates' movement on the actin cytoskeleton, the model was added with an interpretation of how the actin filaments could affect the dynamics of damaged proteins. In this case, if the aggregates were at a distance d_s of the boundaries and in the region where their center's projection to the ' x ' axis lied between the projections to the ' x ' axis of the mother's and the daughter's centers (figure 2.5), the following happened. With a probability P_s and for an exponentially distributed time T_s (with parameter λ_s), the aggregate's walk was altered according to the two ways explained below. In the first one, the proteins would remain still. In the second one, in case of adhesion to the actin filaments while inside the daughter, the aggregate would be transported in direction of the mother cell with a rate v_s through the region with actin-filament presence.

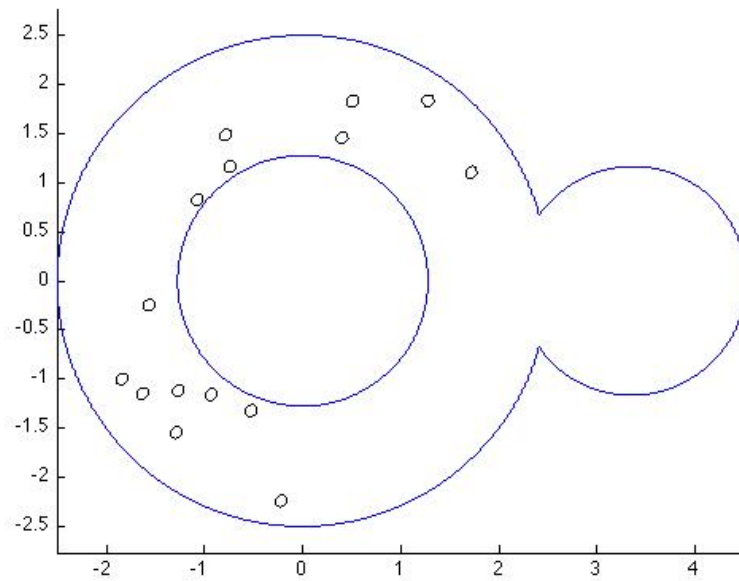


Figure 2.4: $0.12 \mu\text{m}$ diameter aggregates undergoing a random walk inside a $5 \mu\text{m}$ cell (with a $2.55 \mu\text{m}$ vacuole) and a growing bud connected by a $1.35 \mu\text{m}$ neck.

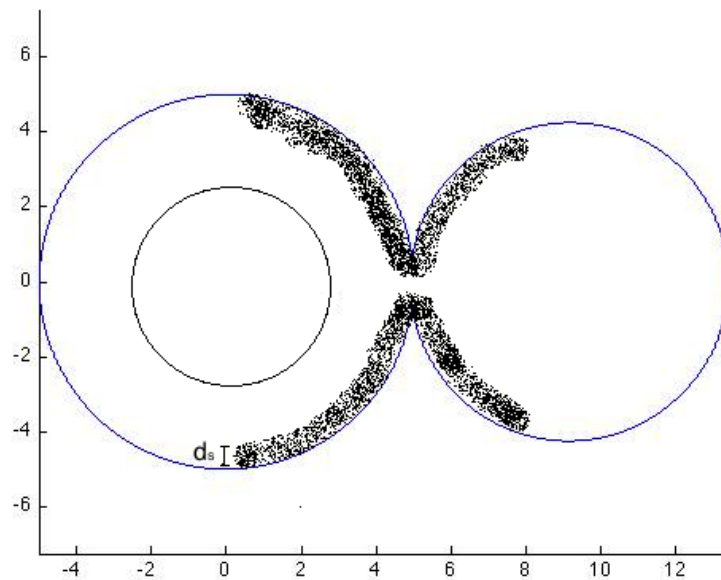


Figure 2.5: Region in the simulated yeast cells where the aggregates' movement is affected by the actin cytoskeleton.

2.2.3 Three-Dimensional Simulations of Diffusion

The three-dimensional simulations of the dynamics of Hsp104-associated aggregates were done as an extension to the two-dimensional ones. The motivation for them was based on our intuition that the probability of a daughter cell having at least one aggregate after yeast cytokinesis could depend on the dimensionality of the model. Also, as it will be seen in the following section, in the case of confined diffusion, the mean-square-displacement's relation to the dimension of the model is not linear.

The three-dimensional programs written for this project model budding yeast cells in a very similar way as those in the previous section. The parameter values remained constant and the aggregates were initialized randomly inside a sphere (representing the mother cell) and were allowed to diffuse inside both it and another sphere (the daughter) connected by a neck. Every time step δt of duration 5 seconds, the aggregates moved from a position (x, y, z) to a position $(x + \chi_1, y + \chi_2, z + \chi_3)$ where χ_1 , χ_2 , and χ_3 are gaussian numbers with mean 0 and variance $\sqrt{2D\delta t}$. The boundary conditions were adapted to their three-dimensional equivalent with the remaining condition that the angle of incidence is equal to the angle of reflection. Constraints such as the vacuole (another sphere inside the mother cell blocking the aggregates movement) and the growing daughter were added progressively to study their effect on the mean-square-displacement of the aggregates and the probability of the daughter cell to inherit at least one damaged protein. Figure 2.6 shows a picture of the geometry in which the aggregates diffuse in the three-dimensional simulations. Additionally, as in the two-dimensional simulations, the programs were altered so that the aggregates undergo subdiffusion instead of a regular random walk. For it, once more, 30% of the aggregates were not allowed to go further than $0.5 \mu\text{m}$ of their initial position.

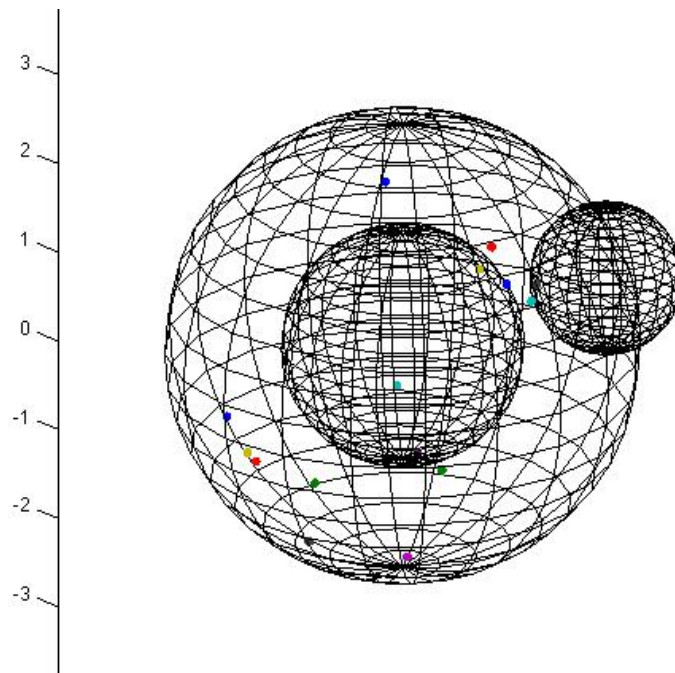


Figure 2.6: Instant picture of the simulation where the aggregates undergo a random walk inside a $5 \mu\text{m}$ diameter yeast cell (with a vacuole) and a growing daughter cell. Both represented by a sphere.

3

Results

IN THE PREVIOUS CHAPTER, the simulations designed to model the motility of Hsp104-associated aggregates were described. Their purpose: finding the possible explanations of both the abnormality in the mean-square-displacement of the damaged proteins and their asymmetric distribution during yeast cytokinesis. Recall that in [13] the mean-square-displacement of damaged proteins during cell cytokinesis was measured. The results, when averaging over more than 1,000 trajectories are shown in the figures in [13]. Also, the experiments performed by [4] show that only 30% of the newborn yeast cells inherit at least one damaged protein. These two measurements will be the guidance when considering if the simulations are successful or not as models of the behavior of Hsp104-associated aggregates during yeast budding.

3.1 Random Walk in x-y Plane

The mean-square-displacement of an aggregate undergoing a random walk in the $x - y$ plane should be equal, when averaged over many trials, to $4Dt$ where D is the diffusion constant. For $D = 0.0005 \mu m^2/sec$ the mean-square-displacement from the simulations, as a function of time t , is shown in figure 3.1.

3.2 Diffusion Inside a Circle

The diffusion equation in polar coordinates r, θ is computed in Appendix A. It has the form

$$\frac{\partial Q}{\partial t} = D \left(\frac{\partial^2 Q}{\partial r^2} + \frac{1}{r} \frac{\partial Q}{\partial r} + \frac{1}{r^2} \frac{\partial^2}{\partial \theta^2} \right). \quad (3.1)$$

In this case, since we are no longer considering a model with only one particle, Q no longer denotes the probability of a particle to be in position (r, θ) after a time t but the

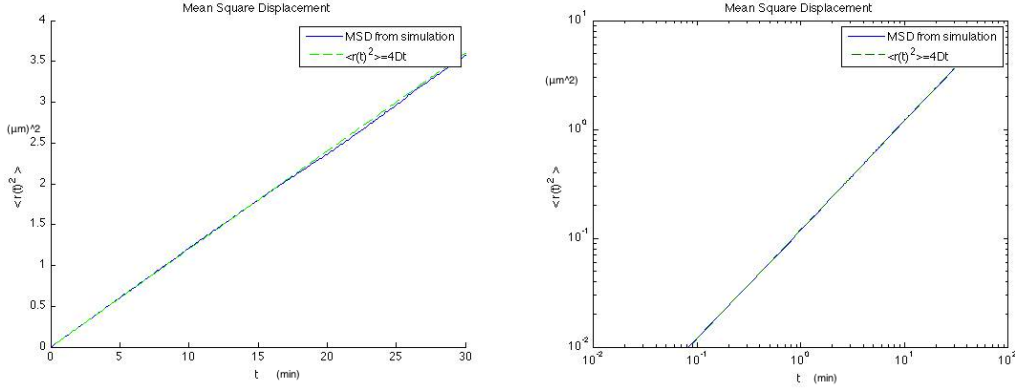


Figure 3.1: Plot and log-log plot of the mean-square-displacement $\langle r(t)^2 \rangle$ of simulated a particle undergoing a random walk in the $x-y$ plane together with the function $f(t) = 4Dt$. Results averaged over 20,00 simulations.

concentration of the particles at the point (r, θ) . The correspondance however, between the two concepts expressed by the function Q is enough to maintain the same notation for both of them.

In [10], the exact expressions of the solution of the diffusion equation in a circle of radius a and the mean-square-displacement of a particle initiated randomly and diffusing inside of it are shown. If $J_i(x)$ denotes the i -th Bessel function of the first kind, $\beta'_n s$ are the zeros of $J'_1(x)$ and a , as explained, is the radius of the circle, then,

$$\langle r^2(t) \rangle = a^2 \left(1 - 8 \sum_n \exp\left(\frac{-\beta_n^2 Dt}{a^2}\right) \frac{1}{\beta_n^2 - 1} \frac{J_0^2(\beta_n)}{J_1^2(\beta_n)} \right). \quad (3.2)$$

As it is seen in the log-log plot in figure 3.3 at short time scales the mean-square-displacement resembles that of regular unconstrained diffusion. At longer time scales, however, it bends until it fixes around a constant value (the radius of giration squared of the geometry of confinement).

Figures 3.3 and 3.4 show the relation between the analytical solution to the mean-square-displacement found in equation 3.2 and the numerical one measured in the simulations. The first one corresponds to a particle diffusing inside a circle of radius $0.0005 \mu\text{ m}$, and the second one of an aggregate, represented by a disc with radius $0.06 \mu\text{ m}$, undergoing diffusion inside a cell of radius $2.5 \mu\text{ m}$. In both cases the difference between both approaches is almost indistinguishable.

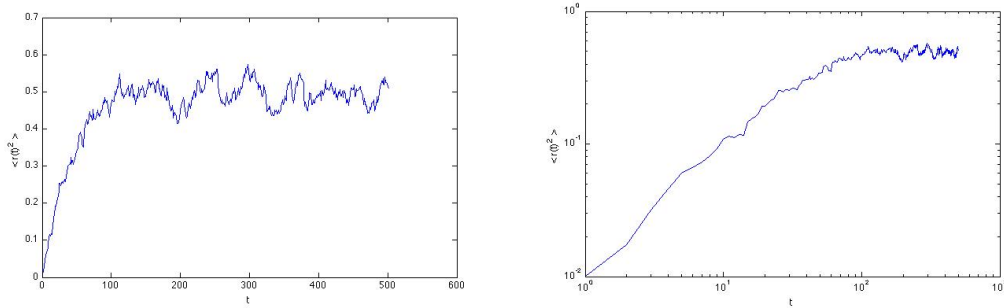


Figure 3.2: Plot and log-log plot of the mean-square-displacement (in of μm^2) as a function of time (in seconds) for a particular simulation of a particle undergoing a random walk inside a circle of radius $1 \mu m$ with the diffusion constant D equal to $0.0005 \mu m^2/sec$ and the time step δt equal to 5 seconds.

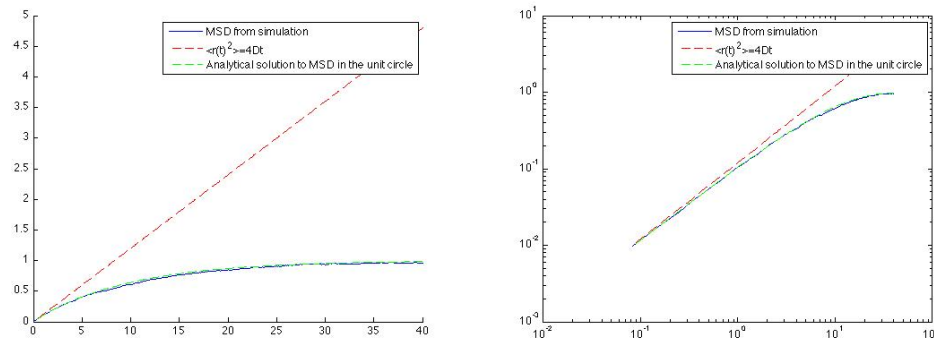


Figure 3.3: Plot and log-log plot of the mean-square displacement as a function of a non-dimensional particle diffusing inside a circle of radius $a = 1 \mu m$. Results averaged over 10,000 simulations. The blue line corresponds to the mean-square-displacement received in the simulation, the dashed line corresponds to the analytical solution to the mean-square-displacement shown in equation 3.2, and the green one to the expect behavior in the case of diffusion with no constraints. .

3.3 Diffusion Inside an Annulus

The yeast cell with vacuole, projected into a two-dimensional plane, can be numerically modeled as an annular-shaped region. Thus, the diffusion equation's solution in an annulus with inner radius a and outer radius b should provide an analytical guidance to how the two-dimensional mean-square-displacement of the aggregates in the simulations, should generally behave. In this case the boundary conditions should be taken as $Q(a, \theta, t) = Q(b, \theta, t) = 0$. The solution to the diffusion equation inside the annulus (See Appendix A), with the initial distribution taken to be a uniform, is derived using the

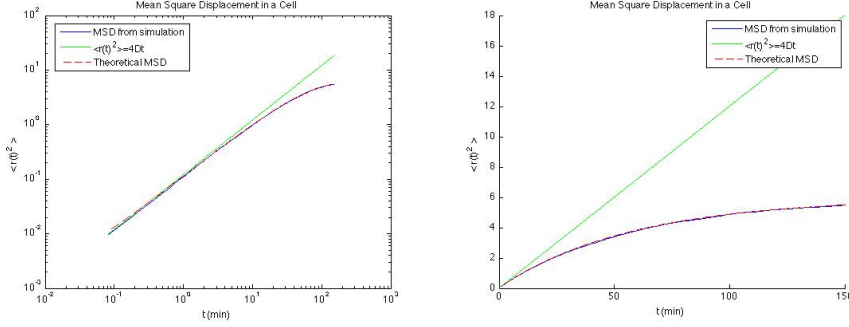


Figure 3.4: Plot and log-log plot of the mean-square-displacement as a function of time of the aggregates with radius $r_a = 0.06 \mu m$ diffusing inside a cell of radius $r_c = 5 \mu m$. Results averaged over 10,000 simulations. The blue line corresponds to the mean-square displacement received in the simulation, the dashed line corresponds to the analytical solution to the mean-square-displacement shown in equation 3.2, and the green one to the expect behavior in the case of diffusion with no constraints.

procedures suggested in [3]. It is

$$Q(r,t) = \frac{\pi^2}{2} \sum_{i=1}^{\infty} \frac{\alpha_i J_0(a\alpha_i)}{J_0^2(a\alpha_i) - J_0^2(b\alpha_i)} \exp(-D\alpha_i^2 t) U_0(r\alpha_i) \int_a^b r f(r) U_0(r\alpha_i) dr \quad (3.3)$$

Notice that the solution has no dependence on the angle. This happens as a result of the initial conditions. As in the appendix, the mean-square-displacement can be computed as

$$\langle r^2(t) \rangle = C(1 - \exp(-2\beta Dt))$$

where C and β are constants. In fact, C is the radius of giration squared as explained in [10]. Figure 3.5 shows the results for the mean-square-displacement in the case of diffusion inside a yeast cell with a vacuole (represented by an annulus).

3.4 Simulations of Hsp104-Associated Aggregate Diffusion in yeast cytokinesis

In this section I will describe the results of the two-dimensional and three-dimensional programs simulating regular diffusion of Hsp104-associated aggregates during yeast budding with and without constraints such as the vacuole and the growing bud. In the two-dimensional case where the mother cell and the bud are both represented by two fixed circles (no vacuole and no growing daughter) the probability P , averaged over 5,000 iterations, of a daughter cell having at least one protein aggregate after yeast cytokinesis is complete is 0.834. On the other hand, In the case of a growing bud and no vacuole P is 0.8154. Finally, when the mother had a vacuole and the daughter grows, P rises to 0.8724. On the other hand, for the three-dimensional models the values of P , in the same order, are 0.682, 0.647, and 0.791. These probabilities are considerably higher than

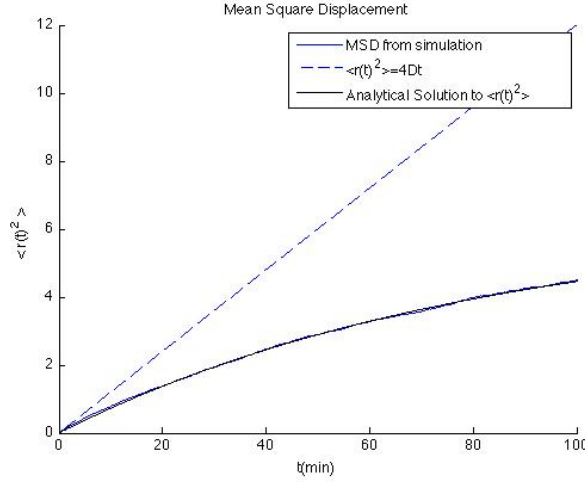


Figure 3.5: Plot of the mean-square-displacement as a function of time of the aggregates with radius $r_a = 0.06 \mu m$ diffusing inside a cell of radius $r_c = 5 \mu m$ with vacuole of radius $r_v = 2.55 \mu m$. Results averaged over 10,000 simulations. The blue line corresponds to the mean-square-displacement obtained in the simulation, the dashed line corresponds to the analytical solution to the mean-square-displacement shown in equation 3.3, and the green one to the expect behavior in the case of diffusion with no constraints.

those observed experimentally (around 0.3 as stated in [4]), thus, the program simulating only diffusion of aggregates can not be considered succesful as a model of the dynamics of the damaged proteins during yeast cytokinesis.

3.5 Remake of Simulations in [13]

In the previous chapter the approach done in [13] was described. In summary, the mean-square-displacement of the protein aggregates during yeast cytokinesis was measured and compared to simulations of diffusion and subdiffusion of protein aggregates during yeast budding. The simulations performed in [13] have the following structure. 80,000 aggregates are initiated randomly in a sphere (a circle in the two-dimensional case) joined to another one by a neck. The positions of the aggregates are updated in the exact same way as in the simulations done for this project, described in detail in the previous chapter. Also, the boundary conditions are taken to be same. The main differences however, between the simulations in [13] and the ones performed here, are that, first, the simulations done in [13] model diffusion with traps (a fraction of the aggregates are not allowed to go further than a previously set distance) instead of regular confined diffusion. Likewise, the simulations done for this project incorporate the vacuole as an additional constraint. Finally, their simulation aims only to study the mean-square-displacement and the concentration of the aggregates while the ones done here measure the above introduced probability P as well. To study if the approach in the article is convincing or not, simulations with the same structure as those in [13], were ran for this

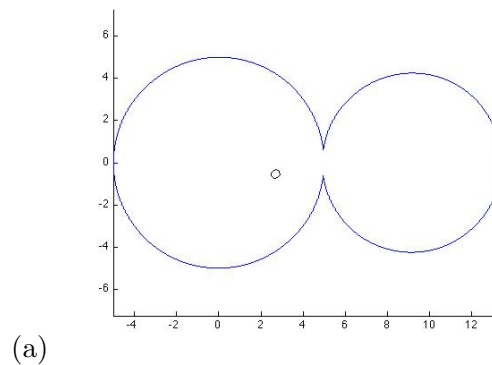


Figure 3.6: (a) $5\mu m$ cell and $4.5\mu m$ bud connected by a bud as in the simulations performed by [13].

project. The main difference however, is that the probability P of a daughter cell having at least one damaged proteins after yeast cell division is complete, is also measured in my programs.

3.5.1 Two-dimensional simulations

As introduced above, in this project the two-dimensional simulations of aggregate subdiffusion done in [13], were repeated in order to study how P behaved under the conditions imposed by the authors of the document. In the simulations done here, as in the ones from the article, the diffusion constant D was taken to be $0.0005\mu m^2/sec$ and the mother's and daughter's diameters were taken to be $5\mu m$ and $4.5\mu m$. In [13] the aggregates walk is classified as subdiffusion. To simulate this process, the approach done both here and in [13] is the following: 30% of the aggregates were not allowed to travel further away than $0.5\mu m$ from their initial positions. Figure 3.6 shows an image of the region in which the aggregates diffuse or subdiffuse in the simulations done in this project it should be compared with the images of the ones performed in [13].

The mean-square-displacement as a function of time calculated in the simulations can be seen in figure 3.7.

To verify if the simulations done in [13] were reliable, the previous program, of which the structure had been copied from the article, was altered in such a way that it could measure P . Also, two other constraints; the vacuole and the growing-bud, were added. When the bud size was fixed and the cell had no vacuole P was 0.686, in the case of a growing bud P was 0.67943, and when the daughter cell had a vacuole and the bud grew P was 0.7558. The mean-square-displacement as a function of time, in each separate case, is shown in figure 3.8.

3.6. SIMULATIONS OF HSP104-SSOCIATED AGGREGATE DIFFUSION IN YEAST CYTOKINESIS IN THE PRESENCE OF ACTIN CYTOSKELETON RESULTS

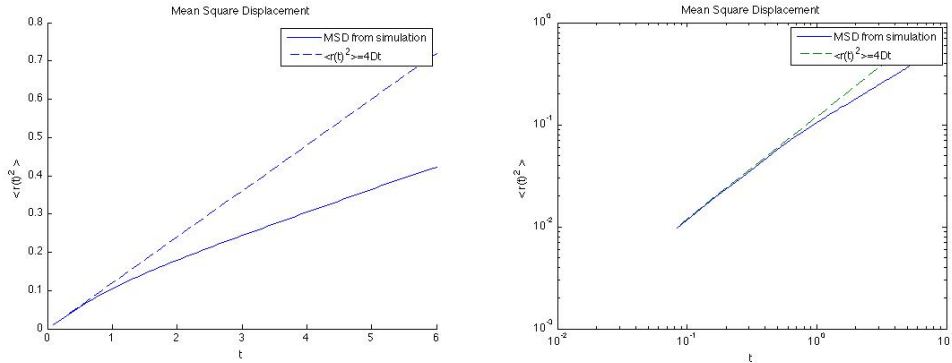


Figure 3.7: Plot and log-log plot of our mean-square-displacement as a function of t when remaking the simulations done in [13] in two-dimensions

3.5.2 Three-dimensional simulations

To verify that the difference between the probability P measured in the previous simulations and the one observed in the experiments in [4] was not entirely due to the dimensionality of the simulated model, 3-d simulations of the same characteristics were done. In this case (under the same parameter values as in the two-dimensional model), the values of P were: 0.4391 for the case where the bud size was fixed, 0.3981 when the bud grew and the mother cell had no vacuole, and 0.4218 when the cell had a vacuole and the bud grew. The mean-square-displacement from the simulations corresponding to the first case is shown in figure 3.9.

3.6 Simulations of Hsp104-ssociated aggregate diffusion in yeast cytokinesis in the presence of actin cytoskeleton

The results of the probability P on a daughter cell having at least one damaged protein-aggregate after yeast cell division is complete are shown in Appendix B. Recall that in this program if the aggregates undergo a random walk in the region shown in figure 2.5 their movement would be altered with a probability P_s for an exponentially distributed time T_s with mean $\frac{1}{\lambda_s}$. For this particular program the values of d_s , P_s , λ_s were varied yielding more than 60 possible arrangements, each of them having a distinct value of P and different behaviors of the mean-square-displacement. For some choices of the three parameters the results matched the experimentally observed. However, the model remains two arbitrary and unrealistic to be considered an appropriate model of yeast cytokinesis.

3.6. SIMULATIONS OF HSP104-ASSOCIATED AGGREGATE DIFFUSION IN YEAST CYTOKINESIS IN THE PRESENCE OF ACTIN Cytoskeleton RESULTS

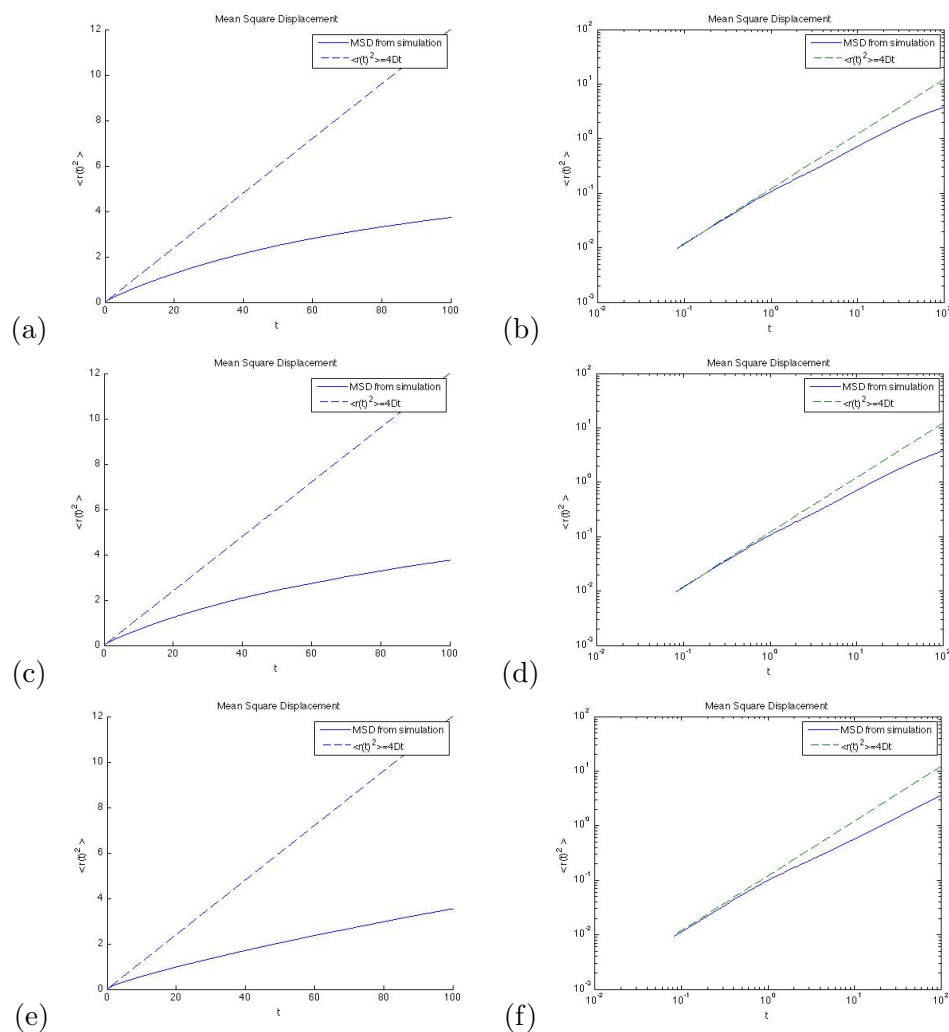


Figure 3.8: (a,b)(c,d)(e,f) Plot and log-log plot of the mean-square-displacement as a function of time of simulated aggregates undergoing diffusion with traps (a fraction of the aggregates are not allowed to travel more than set distance) in a model where the bud size is fixed, the bud is growing and where the bud is growing and the mother cell has a vacuole. Results averaged over 10,000 repetitions.

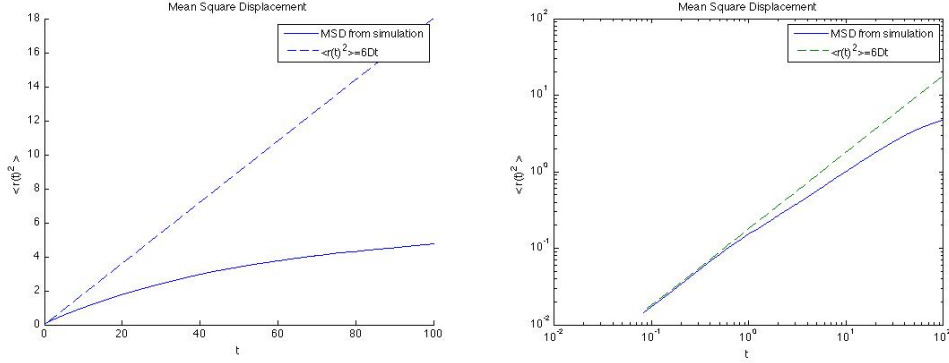


Figure 3.9: Plot and log-log plot of the mean-square-displacement as a function of t when remaking the simulations done in [13] in three-dimensions.

3.7 Comparison to Experiments

The results obtained in both the two-dimensional and the three-dimensional simulations performed for this project can be compared to the experimental observations in two different ways. The first one consists of comparing the likeliness of yeast daughter cells to inherit at least one damaged protein aggregate after yeast cell division is complete (what we called before P). The observations of living yeast cells show that this value is approximately 0.3 which is considerably lower than that obtained in the simulations of diffusion and subdiffusion of aggregates in both three and two dimensions. The lowest value obtained in this simulations was 0.3981 in the three-dimensional model where the aggregates undergo subdiffusion and the bud is continuously growing.

On the other hand, when comparing both the mean-square-displacement obtained in the simulations modelling regular diffusion and the one measured empirically in [13] the result was the following. Generally, simulated values of the mean-square-displacement rose faster, as t increased. In the case of simulated subdiffusion or diffusion with traps, the mean-square-displacement of the aggregates resembled that shown in the results of [13] considerably more. Figure 3.10 shows the mean-square-displacement from the three-dimensional simulations of subdiffusion with and without the vacuole constraint. These pictures must be compared to those in [13]. As it can be seen, specially in the case of the simulations of diffusion with traps inside a yeast cell with a vacuole, the behaviors of both the experimentally observed (in [13]) and simulated mean-square-displacement is almost identical from 0 to 5 minutes. Results beyond that time threshold are not shown in [13], making it impossible to verify if the simulated mean-square-displacement continues to resemble that seen in live-yeast cells.

As it will be later explained in the conclusions, the results obtained from the three-dimensional simulations of aggregate subdiffusion inside a yeast cell with a vacuole (the most reliable simulation), can be analyzed in two different ways. Though it models the mean-square-displacement in a very successfully way, it fails to segregate the aggregates

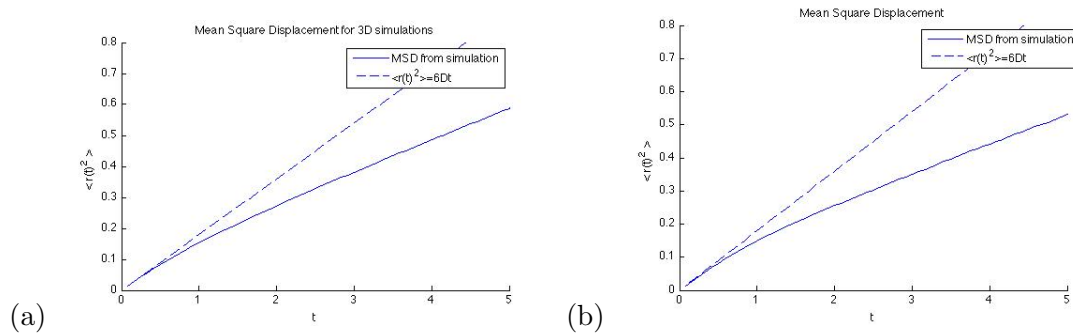


Figure 3.10: (a) Plot of the mean-square-displacement as a function of t when remarking the simulations done in [13] in three-dimensions. Results averaged over 2,000 simulations. (b) Plot of the mean-square-displacement as a function of time t when remarking the simulations performed in [13]. with the vacuole in the mother cell as additional constraint for the diffusion of the aggregates. Results averaged over 2,000 simulations.

asymmetry as in live yeast-cytokinesis. Hence, It would then be precipitated to proclaim the model as a reliable explanation to the asymmetrical inheritance of Hsp104-associated aggregates as it was done in [13]. The difference in the simulated and the measured values most likely exhibits a miscomprehension of the dynamics of the aggregates (the aggregates might not be undergoing an unbiased random walk) or an inaccuracy in the experiments.

4

Conclusion

IN THIS SECTION, the simulations and their results will be analyzed in detail. Based on how much the results resemble those observed in the experiments, the models will be considered either reliable or not as possible representations of the dynamics of Hsp104-associated aggregates during yeast cytokinesis. Recall that the simulations modelled diffusion and subdiffusion (slow diffusion) of damaged protein aggregates during yeast budding. Subdiffusion was modeled as in [13]. The simulations measured the mean-square-displacement of the aggregates as a function of time and the probability P of a daughter cell to have at least one of the aggregates after cell division was over (100 minutes). The probability P and the mean-square-displacement had been measured empirically in [4] and [13]. The results showed that P was approximately 0.3 and the behavior of the mean-square-displacement as a function of time is shown in the figures in [13].

The simulations performed in [13], aimed to classify the dynamics of Hsp104-associated aggregates during yeast cytokinesis. In this article it is concluded that the experimentally measured mean-square-displacement agrees with that of a simulated model of subdiffusion in which the aggregates are initiated inside a sphere that is connected to another one by a neck. Additionally, it is verified that, under these conditions, in the simulation the concentration levels on each of the spheres is different throughout the entire process. To decide whether or not the simulations in [13] are trustworthy, the same simulations were repeated in this project. As an additional attribute, they were altered in such a way that they could measure P (as defined above). In the results obtained (figures 3.10(a) and (c)) one can notice that the mean-square-displacement obtained from the program which copied the structure of that in [13] is not exactly the same as that observed experimentally in the same article. Notice that the mean-square-displacement obtained from my simulations after 5 minutes is above $0.6 \mu m^2$, while the one from the experiments in [13] lies between $0.5 \mu m^2$ and $0.6 \mu m^2$. This difference is diminished, though, when

considering the vacuole inside the mother cell as a part of the program (figures 3.10(a) and (b)). However, this is not the only inconsistency with the simulations copying the structure of those in [13]. Regardless of the presence of the vacuole in the model, P was always above 0.4; a value considerably higher than the one measured when observing living yeast cells. The two aspects exposed above question the veracity of either the simulations or the experiments conducted in [13]. Hence, the conclusion from the article -that aging in yeast cells is purely stochastic- should also be revised.

Another aspect worth analyzing more deeply is if, unlike other substances in the cytoplasm, the damaged protein aggregates do not diffuse. In the results chapter it was seen that the different values of P , when protein aggregates were undergoing regular diffusion and subdiffusion, were always too high in comparison to those observed in the laboratory investigations. Also, the mean-square-displacement as a function of time obtained from the simulations rose faster, in almost all cases, than the one measured in [13]. Thus, the “benfing off” of the mean-square-displacement measured in living yeast cells is unlikely to happen uniquely as a consequence of the geometry of the system. Hence, as it is done in [11], one must ask himself if proteins actually diffuse inside yeast cells or are moving with a different behavior. In case damaged protein aggregates are in fact undergoing diffusion in the cytoplasm then there must be, in accordance to the simulations, either more constraints to their movement or a mechanism impeding them to pass to the daughter cell (actin cytoskeleton). On the other hand, if the proteins are not undergoing diffusion, one must redo the simulations incorporating the new characteristics of the system in seek of concordance with the experimental measurements.

Continuing the previous analysis, a mechanism that could be worth studying more deeply is the dependance of the aggregates movement in the actincytosketon. Although the simulations done for this project were too arbitrary in the selection of parameters (d_s , λ_s , P_s) there were many configurations that gave very accurate results. This indicates the strong potential of this hypothesis. For these simulations to become more reliable, the mean-square-displacement must be approximated again as a function of time as done in [13] with the certainty however that the measurements are not being biased by the methods used in the experiments. Also, some characteristics of the actin-transport (the velocity, the probability of it happening, and the regions in which it is evident) must be approximated in order to build a realistic model. Simulations, as mentioned before, may help to verify if a plausible explanation for the given problem can be considered as reliable or not.

Finally, to conclude this text, the open questions, serving as suggestions to what should be done next, will be exposed. In the first place, the mechanism causing the asymmetry of the aggregates yet remains elusive. As mentioned before, if the geometry and slow diffusion (subdiffusion) of the damaged protein aggregates are unlikely to cause it, then what is? Is the hypothesis formulating Hsp104-associated aggregate transport by the actin cytoskeleton consistent with the experimental observations? If so, how can

this be modeled in an effective and appropriate way? Can the model done for this project serve as starting point?

Bibliography

- [1] Berg, H. C. 1992, Random Walk in Biology. Princeton University Press; 2 edition (July 1, 1992).
- [2] Bickel, T. 2007, Physica A Statistical Mechanics and its Applications, 377, 24 .
- [3] Carslaw, H. S., and J. C. Jaeger. 1959. Conduction of Heat in Solids. 2nd ed. Clarendon Press, Oxford, UK.
- [4] Erjavec N., Nyström T. 2007. Sir2p-dependent cytoskeleton formation and mitotic segregation of damaged proteins - a process regulating the antioxidant capacity of yeast daughter cells. Proc. Natl Acad. Sci. USA 104, 10 877-10 881.
- [5] Folland G.B 1992. Fourier Analysis and Its Applications. Pacific Gove, Calif: Wadsworth and Brooks/Cole Advances Books and Software.
- [6] A. Kusumi, Y. Sako and M. Yamamoto (1993). Confined lateral diffusion of membrane receptors as studied by single particle tracking (nanovid microscopy). Effects of calcium-induced differentiation in cultured epithelial cells. Biophysical Journal, Volume 65, Issue 5, 2021-2040, 1 November 1993.
- [7] Introduction to aging and asymmetric segregation of damage in yeast (*Saccharomyces cerevisiae*). Presentation by Nyström T.
- [8] Saxton, M. J. (1994) Anomalous diffusion due to binding: A Monte Carlo study. Biophys. J. 70, 1250-1262.
- [9] Saxton, M. J. (1994) Anomalous diffusion due to obstacles: A Monte Carlo study. Biophys. J. 66, 394-401.
- [10] Saxton, M. J. (1993) Lateral diffusion in an archipelago: Single-particle diffusion. Biophys. J. 64, 1766-1780.
- [11] Spokoini, Moldavski, Schuldiner, England, and Kaganovich (2012). Confinement to organellar surfaces explains anomalous diffusion and asymmetric inheritance of Hsp104-associated aggregate inclusions. Unpublished.

- [12] Wu, W. (2004). Fourier Series and Fejer's Theorem.
- [13] Zhou, C., Slaughter, B. D., Unruh, J. R., Eldakak, A., Rubinstein, B., and Li, R. (2011). Motility and segregation of Hsp104-associated protein aggregates in budding yeast. *Cell* 147, 1186-1196.

A

Diffusion in Confined Spaces

IN THIS section we will derive the diffusion equation in polar coordinates and then solve it in an annular-shaped region with inner radius a and outer radius b .

A.1 Diffusion Equation in Polar Coordinates

Let $Q(t,x,y)$ denote the concentration at a point (x,y) at time t . The diffusion equation in two dimensions has the form

$$\frac{\partial Q}{\partial t} = D(\Delta Q) \tag{A.1}$$

where,

$$\Delta Q = \frac{\partial^2 Q}{\partial x^2} + \frac{\partial^2 Q}{\partial y^2}$$

is the laplacian of the function Q . In the following lines we will derive the laplacian in polar coordinates.

Let $x = r \cos \theta$, $y = r \sin \theta$. Notice that

$$\begin{aligned} \frac{\partial Q}{\partial r} &= \frac{\partial Q}{\partial x} \frac{\partial x}{\partial r} + \frac{\partial Q}{\partial y} \frac{\partial y}{\partial r} = \cos \theta \frac{\partial Q}{\partial x} + \sin \theta \frac{\partial Q}{\partial y} \\ \frac{\partial Q}{\partial \theta} &= \frac{\partial Q}{\partial x} \frac{\partial x}{\partial \theta} + \frac{\partial Q}{\partial y} \frac{\partial y}{\partial \theta} = -r \sin \theta \frac{\partial Q}{\partial x} + r \cos \theta \frac{\partial Q}{\partial y}. \end{aligned}$$

Solving this system for $\frac{\partial Q}{\partial x}$ and $\frac{\partial Q}{\partial y}$ yields

$$\begin{aligned} \frac{\partial Q}{\partial x} &= \cos \theta \frac{\partial Q}{\partial r} - \frac{\sin \theta}{r} \frac{\partial Q}{\partial \theta} \\ \frac{\partial Q}{\partial y} &= \sin \theta \frac{\partial Q}{\partial r} + \frac{\cos \theta}{r} \frac{\partial Q}{\partial \theta} \end{aligned}$$

Let $F := \frac{\partial Q}{\partial x}$ and $G := \frac{\partial Q}{\partial y}$. Since we made no assumption on the particular form of Q we have that F and G also satisfy

$$\begin{aligned}\frac{\partial F}{\partial x} &= \cos \theta \frac{\partial F}{\partial r} - \frac{\sin \theta}{r} \frac{\partial F}{\partial \theta} \\ \frac{\partial G}{\partial y} &= \sin \theta \frac{\partial G}{\partial r} + \frac{\cos \theta}{r} \frac{\partial G}{\partial \theta}\end{aligned}$$

Hence,

$$\frac{\partial^2 Q}{\partial x^2} + \frac{\partial^2 Q}{\partial y^2} = \frac{\partial F}{\partial x} + \frac{\partial G}{\partial y} = \cos \theta \frac{\partial F}{\partial r} - \frac{\sin \theta}{r} \frac{\partial F}{\partial \theta} + \sin \theta \frac{\partial G}{\partial r} + \frac{\cos \theta}{r} \frac{\partial G}{\partial \theta}. \quad (\text{A.2})$$

We then just need to find the partial derivatives of F and G with respect to r and θ .

$$\begin{aligned}\frac{\partial F}{\partial r} &= \cos \theta \frac{\partial^2 Q}{\partial r^2} - \frac{\sin \theta}{r} \frac{\partial^2 Q}{\partial r \partial \theta} + \frac{\sin \theta}{r^2} \frac{\partial Q}{\partial \theta}, \\ \frac{\partial G}{\partial r} &= \sin \theta \frac{\partial^2 Q}{\partial r^2} + \frac{\cos \theta}{r} \frac{\partial^2 Q}{\partial r \partial \theta} - \frac{\cos \theta}{r^2} \frac{\partial Q}{\partial \theta}, \\ \frac{\partial F}{\partial \theta} &= \cos \theta \frac{\partial^2 Q}{\partial \theta \partial r} - \sin \theta \frac{\partial Q}{\partial r} - \frac{\sin \theta}{r} \frac{\partial^2 Q}{\partial \theta^2} - \frac{\cos \theta}{r} \frac{\partial Q}{\partial \theta} \\ \frac{\partial G}{\partial \theta} &= \sin \theta \frac{\partial^2 Q}{\partial \theta \partial r} + \cos \theta \frac{\partial Q}{\partial r} + \frac{\cos \theta}{r} \frac{\partial^2 Q}{\partial \theta^2} - \frac{\sin \theta}{r} \frac{\partial Q}{\partial \theta}\end{aligned}$$

Substituting this values in equation A.2 we get

$$\Delta Q = \frac{\partial^2 Q}{\partial r^2} + \frac{1}{r} \frac{\partial Q}{\partial r} + \frac{1}{r^2} \frac{\partial^2 Q}{\partial \theta^2} \quad (\text{A.3})$$

A.2 Diffusion in the Annulus

The diffusion equation in an annulus with inner radius a and outer radius b can be written as

$$\frac{\partial Q}{\partial t} = D \left(\frac{\partial^2 Q}{\partial r^2} + \frac{1}{r} \frac{\partial Q}{\partial r} + \frac{1}{r^2} \frac{\partial^2 Q}{\partial \theta^2} \right) \quad (\text{A.4})$$

with $a < r < b$, and $Q(a, \theta, t) = Q(b, \theta, t) = 0 \forall t, \forall \theta$. however, since the initial conditions formulate that the concentration is uniform at time $t = 0$ we have that $\frac{\partial Q}{\partial \theta} = 0$. Hence, we can simplify the diffusion equation to

$$\frac{\partial Q}{\partial t} = D \left(\frac{\partial^2 Q}{\partial r^2} + \frac{1}{r} \frac{\partial Q}{\partial r} \right) \quad (\text{A.5})$$

Lets assume that $Q(r, t) = R(r)T(t)$. We can transform the diffusion equation to

$$RT' = D(TR'' + r^{-1}TR') \quad (\text{A.6})$$

Separating the terms dependant on the two variables one gets

$$\frac{T'}{T} = D \left(\frac{R''}{R} + \frac{1}{r} \frac{R'}{R} \right)$$

Since T has no dependance on r and R has no dependance on t . This equation must be equal to a constant $-\alpha^2$. Thus, we get two new equations

$$\frac{T'}{DT} = -\alpha^2 \tag{A.7}$$

$$R'' + \frac{1}{r}R' + \alpha^2 R = 0 \tag{A.8}$$

The first differential equation is separable and can be solved as $T(t) = \exp(-D\alpha^2 t)$. The second one, on the other hand is Bessel's function of degree zero. Its solution, taking into account the constraints introduced above, is found in [3] and has the form

$$U_0(\alpha r) = J_0(\alpha r)Y_0(\alpha b) - J_0(\alpha b)Y_0(\alpha r) \tag{A.9}$$

where J_0 , Y_0 are the bessel functions of the first and second kind and α is a root of the equation

$$J_0(\alpha a)Y_0(\alpha b) - J_0(\alpha b)Y_0(\alpha a) = 0. \tag{A.10}$$

This means that Q can be written as

$$Q(r,t) = \sum_i A_i U_0(\alpha_i r) \exp(-D\alpha_i^2 t) \tag{A.11}$$

Let $f(r)$ be the initial distribution. We have then that

$$f(r) = Q(r,0) = \sum_i A_i U_0(\alpha_i r)$$

The coefficients A_i are found to be [3]

$$A_i = \frac{\pi^2 \alpha_i^2}{2} \frac{J_0(a\alpha_i)}{J_0^2(a\alpha_i) - J_0(b\alpha_i)} \int_a^b r f(r) U_0(r\alpha_i) dr.$$

Which means that our solution is

$$Q(r,t) = \frac{\pi^2}{2} \sum_{i=1}^{\infty} \frac{\alpha_i J_0(a\alpha_i)}{J_0^2(a\alpha_i) - J_0^2(b\alpha_i)} \exp(-D\alpha_i^2 t) U_0(r\alpha_i) \times \int_a^b r f(r) U_0(r\alpha_i) dr$$

Recall that the mean square displacement $\langle r^2(t) \rangle$ is defined as

$$\langle r^2(t) \rangle = \int_{-\infty}^{\infty} r^2 Q(r,t) dr$$

This integral is approximated to be ([6])

$$\langle r^2(t) \rangle = C(1 - \exp(-2\beta Dt)) \tag{A.12}$$

where C and β are constants.

B

Results from Simulations with the Possibility for the Aggregates to Attach to the Actin Filaments

AS EXPLAINED IN THE RESULTS CHAPTER, for the program simulating diffusion of protein aggregates with the possibility for them to get trapped in the actin filaments, many simulations were ran using distinct choices for the three parameters d_s , λ_s , and P_s . In this appendix we will show the different values of P resulting from each simulation.

Table B.1: Values of the probability P of an aggregate ending in the bud after 100 minutes for different P_s , λ_s when averaging over 2,000 simulations. In this case $d_s = 0\mu\text{m}$, i.e the aggregates only attach to the boundary, and there is NO displacement of them by the cables.

P_s	$\lambda_s^{-1} = \infty$
1	0.5195
0.75	0.531
0.5	0.569
0.25	0.63

APPENDIX B. RESULTS FROM SIMULATIONS WITH THE POSSIBILITY FOR
THE AGGREGATES TO ATTACH TO THE ACTIN FILAMENTS

Table B.2: Values of the probability P of an aggregate ending in the bud after 100 minutes for different P_s and λ_s when averaging over 2,000 simulations. In this case $d_s = 0\mu\text{m}$, i.e the aggregates only attach to the boundary, and if the aggregates get attached in the daughter cell then they are always dragged towards the mother cell by the actin filaments.

P_s	$\lambda_s^{-1} = \infty$	$\lambda_s^{-1} = 75 \text{ min}$	$\lambda_s^{-1} = 50 \text{ min}$	$\lambda_s^{-1} = 25 \text{ min}$
1	0.0105	0.156	0.245	0.4965
0.75	0.014	0.172	0.2875	0.5495
0.5	0.0505	0.2255	0.328	0.606
0.25	0.06	0.3345	0.455	0.675

Table B.3: Values of the probability P of an aggregate ending in the bud after 100 minutes for different P_s and λ_s when averaging over 2,000 simulations. In this case $d_s = 0.3\mu\text{m}$ and there is NO displacement of them by the cables.

P_s	$\lambda_s^{-1} = \infty$	$\lambda_s^{-1} = 75 \text{ min}$	$\lambda_s^{-1} = 50 \text{ min}$	$\lambda_s^{-1} = 25 \text{ min}$
1	0.186	0.2904	0.46167	0.615
0.75	0.224	0.312	0.498	0.65
0.5	0.2581	0.372	0.539	0.72
0.25	0.29921	0.4289	0.6016	0.798

Table B.4: Values of the probability P of an aggregate ending in the bud after 100 minutes for different P_s and λ_s when averaging over 2,000 simulations. In this case $d_s = 0.3\mu\text{m}$, and if the aggregates get attached in the daughter cell then they are always dragged towards the mother cell by the actin filaments.

P_s	$\lambda_s^{-1} = \infty$	$\lambda_s^{-1} = 75 \text{ min}$	$\lambda_s^{-1} = 50 \text{ min}$	$\lambda_s^{-1} = 25 \text{ min}$
1	0.0056	0.021	0.06	0.0982
0.75	0.0082	0.0423	0.0621	0.1801
0.5	0.015	0.08	0.1174	0.275
0.25	0.0189	0.104	0.1673	0.364